



Since January 2020 Elsevier has created a COVID-19 resource centre with free information in English and Mandarin on the novel coronavirus COVID-19. The COVID-19 resource centre is hosted on Elsevier Connect, the company's public news and information website.

Elsevier hereby grants permission to make all its COVID-19-related research that is available on the COVID-19 resource centre - including this research content - immediately available in PubMed Central and other publicly funded repositories, such as the WHO COVID database with rights for unrestricted research re-use and analyses in any form or by any means with acknowledgement of the original source. These permissions are granted for free by Elsevier for as long as the COVID-19 resource centre remains active.



# Coronavirus Disease 2019 (COVID-19) in Molecular Imaging: A Systematic Review of Incidental Detection of SARS-CoV-2 Pneumonia on PET Studies

Faranak Rafiee, MD,<sup>\*,#</sup> Pedram Keshavarz, MD,<sup>\*,†,#</sup> Sanaz Katal, MD,<sup>‡</sup> Majid Assadi, MD,<sup>§</sup> Seyed Faraz Nejati, MD,<sup>\*</sup> Faranak Ebrahimian Sadabad, MD,<sup>\*</sup> and Ali Gholamrezanezhad, MD, FEBNM, DABR<sup>||</sup>

There have been several reports of the incidental detection of severe acute respiratory syndrome coronavirus 2 pneumonia on positron emission tomography/computed tomography (PET/CT) studies, which represent the potential role of molecular imaging in the detection and management of coronavirus disease 2019. Here, we systematically review the value of PET/CT in this setting. We conducted a systematic search on June 23, 2020, for PET studies with findings suggestive of coronavirus disease 2019. Web of Science, PubMed, Scopus, EMBASE, and Google Scholar databases were used. Patients with at least one PET/CT imaging evaluation were included in the study. Fifty-two patients in 30 publications with a mean age of  $60 \pm 12.74$  (age range; 27-87) were included in this study, of which 28 (53.8%) were male, and 19 (36.5%) were female. In 5 (9.7%) patients, gender was not reported. PET/CT was performed with  $^{18}\text{F}$ -fluorodeoxyglucose for 48 (92.3%),  $^{18}\text{F}$ -choline for 3 (5.8%), and  $^{68}\text{Ga}$ -PSMA for 1 (1.9%) patients. The mean SUV max of pulmonary lesions with  $^{18}\text{F}$ -fluorodeoxyglucose uptake was  $4.9 \pm 2.3$ . Moreover, 39 (75%) cases had an underlying malignancy, including 18 different type of primary cancers and 6 (11.5%) patients with metastatic disease. The most common pulmonary findings in PET/CT were bilateral hypermetabolic ground-glass opacities in 39 (75%), consolidation in 18 (34.6%), and interlobular thickening in 4 (7.6%). In addition, mediastinal 14 (27%) and hilar 10 (19.2%) lymph node involvement with increased metabolic activity was frequently identified. Early diagnosis of severe acute respiratory syndrome coronavirus 2 pneumonia is not only crucial for both appropriate patient management but also helps to ensure appropriate postexposure precautions are implemented for the department and hospital staff and those who have been in contact with the patient.

Semin Nucl Med 51:178-191 © 2020 Elsevier Inc. All rights reserved.

*Abbreviations:* COVID-19, the novel Coronavirus disease; GGOs, ground-glass opacities; PET/CT, positron emission tomography/computed tomography;  $^{18}\text{F}$ -FDG,  $^{18}\text{F}$ -fluorodeoxyglucose;  $^{68}\text{Ga}$ -PSMA,  $^{68}\text{Ga}$ -prostate-specific membrane antigen; SUVmax, maximum standardized uptake values

<sup>\*</sup>Department of Radiology, Medical Imaging Research Center, Shiraz University of Medical Sciences, Shiraz, Iran.

<sup>†</sup>Department of Radiology, Tbilisi State Medical University (TSMU), Tbilisi, Georgia.

<sup>‡</sup>Department of Nuclear Medicine/PET-CT, Kowsar Hospital, Shiraz, Iran.

<sup>§</sup>Department of Molecular Imaging and Radionuclide Therapy (MIRT), The Persian Gulf Nuclear Medicine Research Center, Bushehr Medical

University Hospital, School of Medicine, Bushehr University of Medical Sciences, Bushehr, Iran.

<sup>||</sup>Department of Radiology, Keck School of Medicine, University of Southern California (USC), Los Angeles, CA.

Funding information: The authors state that this work has not received any funding.

Address reprint requests to Ali Gholamrezanezhad, MD, FEBNM, DABR, Department of Radiology, Division of Emergency Radiology, Keck School of Medicine, University of Southern California, 1500 San Pablo Street, Los Angeles, CA 90033. E-mail: [ali.gholamrezanezhad@med.usc.edu](mailto:ali.gholamrezanezhad@med.usc.edu)

<sup>#</sup>Contributed equally to this article.

## Introduction

The novel Coronavirus disease 2019 (COVID-19) caused by severe acute respiratory syndrome coronavirus 2 (SARS-CoV-2 coronavirus), first emerged in China, and then spread to the other regions worldwide.<sup>1</sup> Currently, almost all countries have been seriously affected by the global pandemic, with profound impacts on their healthcare and socioeconomic systems. As of July 23, 2020, a total of 15 million COVID-19 cases with around 630,000 deaths have been confirmed worldwide.<sup>2</sup> COVID-19 typically presents with fever and lower respiratory symptoms, and the majority of infected patients display bilateral multifocal pulmonary lesions in chest imaging. No definitive therapy for the SARS-CoV-2 infection is available yet. Hence, early diagnosis, early isolation, and supportive management continue to be the crucial strategies to combat the present crisis.<sup>3</sup>

Viral RNA nucleic acid testing (RT-PCR) is currently considered the gold standard of diagnosis; however, the test suffers from insufficient sensitivity, particularly in the early time course of the disease.<sup>4,5</sup> Therefore, chest imaging, specifically high-resolution CT, has been purposed as a supportive tool in the detection and management of SARS-CoV-2 pneumonia. Numerous publications have described the major imaging features of COVID-19. Multifocal ground-glass opacities (GGOs) with a peripheral distribution and later superimposition of consolidation are among the most frequently reported characteristics.<sup>6–8</sup> However, the mentioned findings are not highly specific for COVID-19, and several other lung pathologies might also mimic similar CT manifestations.

Moreover, despite some uncertainties due to the lack of enough data, there might be a potential role for other imaging tools (eg, positron emission tomography/computed tomography or PET/CT) in the detection and management of COVID-19.<sup>9</sup> Although <sup>18</sup>F-fluorodeoxyglucose (<sup>18</sup>F-FDG) PET/CT is not usually employed in the diagnosis of acute pneumonia, its clinical value in the pulmonary inflammatory/infectious conditions has already been explored.<sup>10</sup> <sup>18</sup>F-FDG-PET can assess the severity of the disease, monitor disease progression, and evaluate the post-therapy response.<sup>11</sup> More importantly, whole-body PET/CT imaging offers a unique chance to evaluate the possible extrapulmonary manifestations of COVID-19.

Over the last few months, several case reports with incidental detection of COVID-19 on PET/CT have been published worldwide.<sup>12,13</sup> However, a comprehensive study is still lacking in this regard. Hence, we conducted the present study to comprehensively review the available publications on PET/CT findings in COVID-19, which might guide us to a better understanding of the disease pathology, its long-term complications, and developing novel therapies. Indeed, the potential added value of FDG-PET/CT in depicting the underlying pathophysiological inflammatory process might offer a great chance to fight against the ongoing COVID-19 pandemic.

## Materials and Methods

### Search Strategy

We conducted a systematic search for available published articles describing PET findings in COVID-19 patients. The search was performed on June 23, 2020, using Web of Science, PubMed, Scopus, EMBASE, and Google Scholar databases. The following search keywords were used: “COVID-19”, “coronavirus”, “coronavirus and infection”, “SARS-CoV-19”, “2019-CoV-19”, “radiolog\*”, “Tomography, X-ray, Computed”, “Positron-Emission Tomography”, “PET/CT\*”, and “FDG-PET”. The full list of keywords which were used in the databases is provided as Appendix 1. The study flow diagram is also presented in [Figure 1](#).

### Eligibility Criteria

Patients with confirmed COVID-19 infection (by RT-PCR test using nasopharyngeal swabs), with at least one PET/CT imaging evaluation were included in the study. Duplicate studies, conference abstracts, irrelevant reports, and studies in any language except English were excluded.

### Data Extraction and Quality Assessments

Regarding the quality assessment, two independent reviewers assessed the risk of bias of the included studies using the National Institutes of Health quality assessment tool for case series/reports,<sup>14</sup> and cohort studies using the modified version of Newcastle-Ottawa Quality Scale<sup>15</sup> (Supplementary Tables 1 and 2). Two blinded reviewers extracted data and then proceeded to cross-check the results. The third reviewer resolved disagreements via consensus. The following data were extracted: First author’s name, study region, study type, patient’s age, gender, type of cancer or reason for the exam, pulmonary PET/CT imaging findings, extrapulmonary PET/CT imaging findings, maximum standardized uptake values (SUVmax) of the target pulmonary lesions, and the radiopharmaceutical used in PET imaging. Moreover, we reported one patient in our center ([Fig. 2](#)) and collected a series of PET/CT images from three included studies<sup>16–18</sup> via formal permissions obtained from their publishers ([Figs. 3–5](#)).

## Results

### Included Studies

After excluding the duplicate search results and full-text analysis, 30 studies were included in the final review: 19 case reports, three case series, two cohort studies, and six letters to the editor and commentaries. According to the National Institutes of Health and Newcastle-Ottawa Quality Scale quality assessment tools, quality of included studies was predominantly fair (Supplementary Tables 1 and 2). Fifty-two patients with a mean age of  $60 \pm 12.74$  (age range; 27–87, age Interquartile range; 55–67 years old) were included in this study, of which 28 (53.8%) were male, and 19 (36.5%) were female. In 5(9.6%) patients, the gender was not

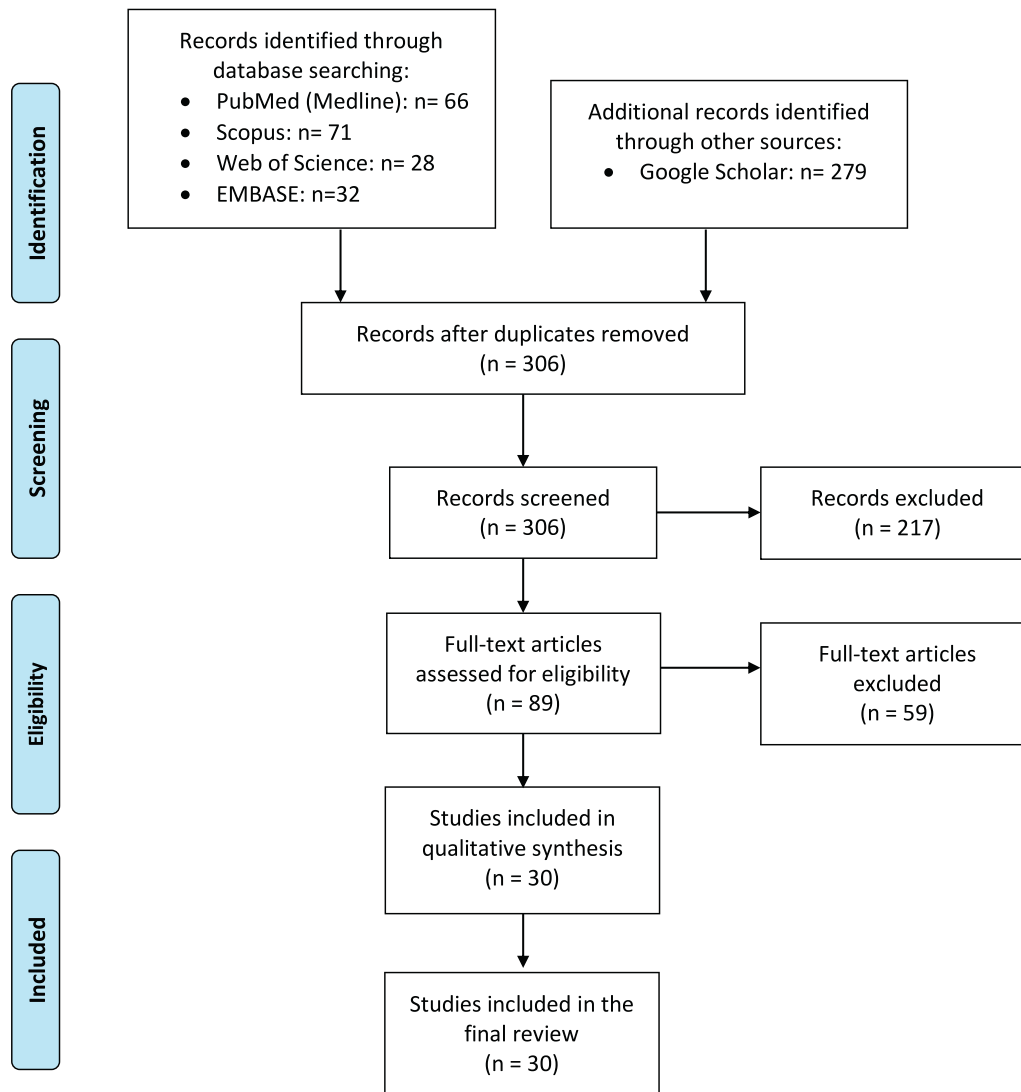


**Figure 1** Flow diagram of study selection process.

reported (Table 1). PET/CT scan was performed with  $^{18}\text{F}$ -FDG for 48 (92.3%),  $^{18}\text{F}$ -choline for 3 (5.8%), and  $^{68}\text{Ga}$ -prostate-specific membrane antigen ( $^{68}\text{Ga}$ -PSMA) for 1 (1.9%) patients. Additionally, one patient (no. 2) had both  $^{18}\text{F}$ -FDG-PET/CT and PET/MR. The mean SUV max of pulmonary lesions with  $^{18}\text{F}$ -FDG uptake was  $4.9 \pm 2.3$ , with a range of 2.2-18. Besides, mildly increased activity of pulmonary lesions was observed on  $^{18}\text{F}$ -choline and  $^{68}\text{Ga}$ -PSMA studies (SUVmax of 3.8 and 3.2, retrospectively). With regard to the patient's chronic disease, 39 (75%) cases had underlying malignancy, including 18 different types of cancer, presented in Table 2. Five (9.6%) patients had metastases to other organs such as bone (n = 2), lung (n = 2) and liver (n = 1).

### PET/CT Findings

The most common pulmonary PET/CT findings were hypermetabolic bilateral GGOs in 39 (75%), followed by consolidation in 18 (34.6%), and interlobular thickening in 4 (7.6%). Moreover, mediastinal 14 (27%), and hilar

10 (19.2%) lymph node involvement with high metabolic activity was frequently seen (Table 3).

Four patients (no. 3, no. 8, no. 21, and no. 51) were discharged from the hospital; patient no. 3 was a known case of Hodgkin's lymphoma, with a history of diabetes and morbid obesity, who was referred for staging PET in an outpatient facility. She did not report any history of recent travel or contact with known cases of COVID-19. The PET/CT showed stage II right pelvic adenopathy with only mild  $^{18}\text{F}$ -FDG activity (SUVmax 2.9). Multifocal bilateral peripheral pulmonary opacities with moderate  $^{18}\text{F}$ -FDG activity (SUVmax 4.5) were identified in the left lower lobe. Two days later, she developed a runny nose, coughing, and fever (38°C). She was discharged uneventfully after 1 week of inpatient management, but her pelvic radiation was postponed due to the restrictions carried out during the COVID-19 pandemic.

Patient no. 8 was a Wuhan resident, who presented to the hospital with diarrhea and vertigo for 2 days. Following detection of GGOs in the upper lobe of the left lung in the chest CT scan,  $^{18}\text{F}$ -FDG-PET/CT was performed to differentiate between benign or malignant etiologies. The maximum

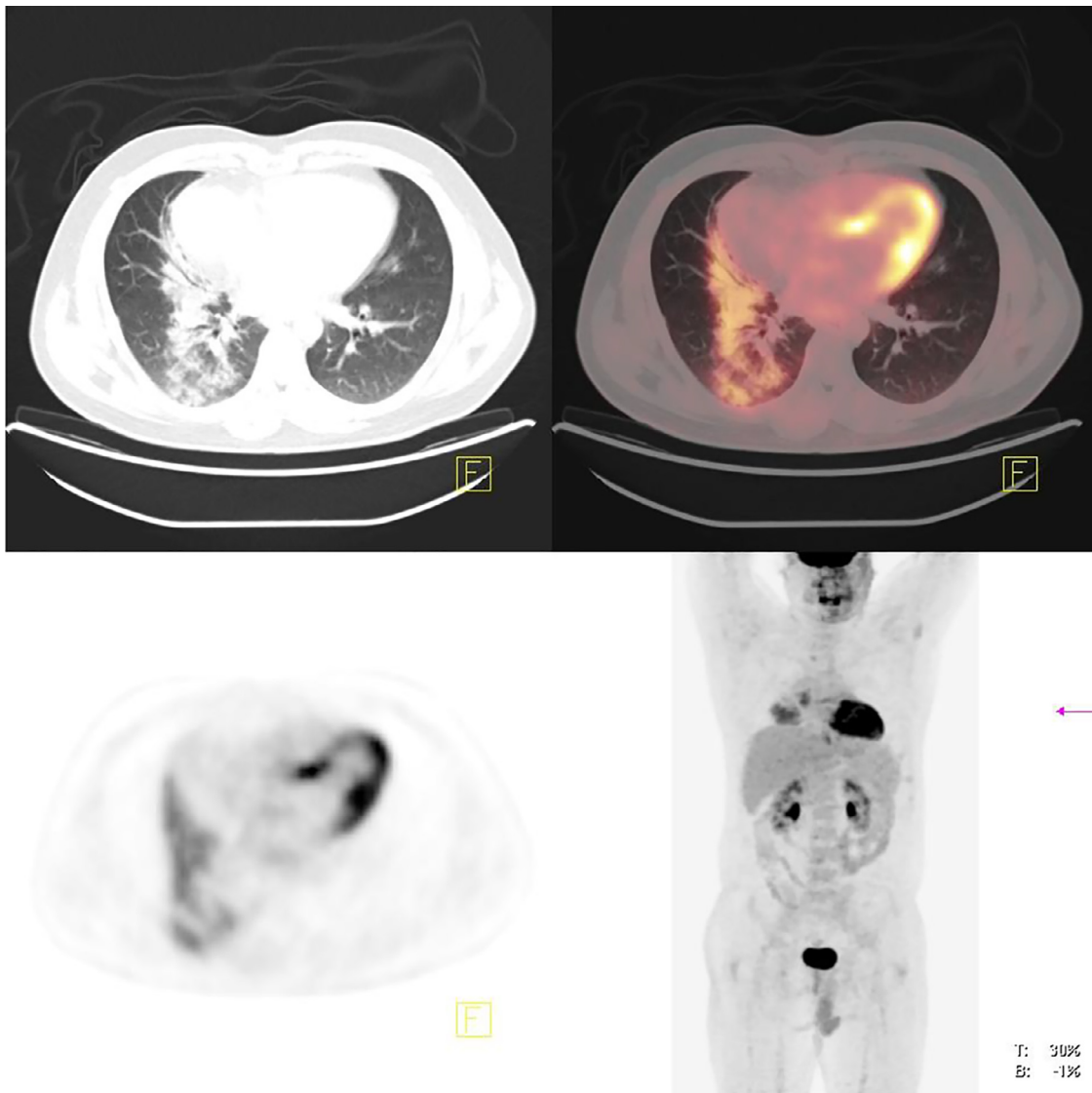


**Figure 2** A 33-year-old male with history of Hodgkin's lymphoma was referred for follow-up post-treatment imaging.  $^{18}\text{F}$ FDG-PET/CT scan revealed mild residual metabolic activity of the mediastinal lymph nodes and focal ill defined hypermetabolic consolidation in right lung base, consistent with atypical pneumonia. The diagnosis of COVID-19 was confirmed by PCR.

intensive projection image showed  $^{18}\text{F}$ -FDG uptake in bilateral lungs, with the SUVmax ranging from 2.4 to 12.4 in lung GGOs. The patient received antibiotics and anti-inflammatory therapy against COVID-19. Follow-up chest CT on day nine of admission demonstrated interval progression of GGOs. Follow-up chest CT on day nineteen of admission demonstrated interval resolution of the previously identified GGOs with minimal residual consolidation. The patient was symptom-free since day 18 and was discharged from hospital on day 30.

Patient no. 51, again from Wuhan, presented with fever, fatigue and dry cough for 5 days. His previous CT suggested hilar malignancy.  $^{18}\text{F}$ -FDG PET/CT showed an FDG-avid mass with a SUVmax of 4.9 in the right lung and increased uptake of FDG in the right paratracheal and right hilar lymph nodes, as well as bone marrow (Fig. 3). First nasopharyngeal

swab test was negative for COVID-19 infections. However, the second RT-PCR test turned positive for COVID-19 and the patient recovered and discharged from the hospital after ten days of admission.

In terms of COVID-related extrapulmonary PET/CT findings, only one patient (no. 34) with anosmia was reported. She was a 27-year-old woman with no respiratory problems, with persistent isolated anosmia for six weeks. PET/CT revealed mild asymmetric hypometabolism in the left orbitofrontal cortex (SUVmax of 9.5 on the left side, in comparison with 10 on the right side). Though, FDG uptake in the left inferior temporal cortex was normal (Fig. 5).

$^{18}\text{F}$ -choline PET/CT was performed for only three patients (no. 22, no. 27 and no. 45). Patient no. 27 was a 59-year-old man with a history of recurrent prostate cancer.  $^{18}\text{F}$ -choline

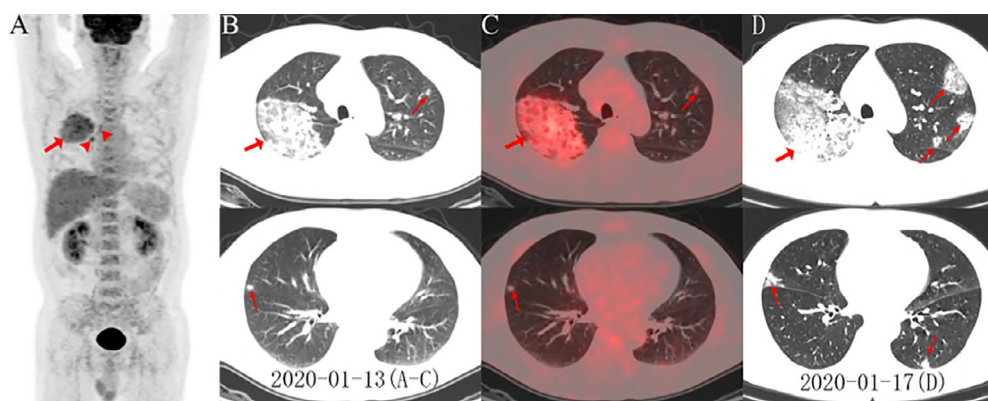


**Figure 3** (A) PET maximum intensity projection (MIP) image of patient no. 51 revealed an FDG-avid mass with a SUV-max of 4.9 in the right lung. Increased accumulation of FDG in the right paratracheal, right hilar lymph nodes (arrowheads), and bone marrow were also noted. On axial images (B, low dose CT; C, PET/CT fusion) there were ground-glass opacities (GGOs) with areas of focal consolidation primarily in the right upper lobe (arrows) and a focal opacity in the left upper and right middle lobes (arrows). Follow-up CT 4-day later demonstrated progression of lesions in bilateral upper and middle lobes with newly developed focal opacities in the left upper and lower lobes (D, arrows). Images obtained from Zou et al,<sup>16</sup> *Radiology*, March 6, 2020 and permission to use granted by Ashley E. Daly, Senior Manager of Radiology, Radiological Society of North America (RSNA).

PET/CT performed after radical prostatectomy for the evaluation of disease spread. This patient had no respiratory symptoms or fever. Choline PET revealed bilateral subsegmental peripheral areas of GGOs with an increased choline-PET uptake (SUV max ranging from 3 to 4). No pleural effusion or mediastinal lymph node involvement was noted. In addition, bone metastases with no pelvic nodal involvement were detected. After 36 hours of choline PET examination, the patient developed dizziness, fatigue, and respiratory failure, and thus was admitted to the hospital.

## Discussion

As COVID-19 continues throughout the world, a variety of imaging findings have been reported. Chest imaging (chest X-ray and CT) has been successfully employed as a practical supplement to RT-PCR testing for COVID-19 diagnosis. Moreover, CT can be used as a valuable tool for evaluation and monitoring of lung lesions in COVID-19. Multiple bilateral GGOs with a peripheral and posterior distribution with or without superimposed consolidations are the typical CT manifestations of SARS-CoV-2 infection in the lungs.

PET imaging is commonly performed for patients with underlying inflammatory or neoplastic disease and guides the therapeutic strategies of these patients by evaluating the extent and burden of the disease and staging. Although based on the available reports, COVID-19 can be detected by PET/CT, several factors might explain why routine molecular imaging does not seem beneficial in the evaluation of COVID-19. PET is generally considered a high-cost imaging modality with prolonged acquisition time. It also has increased radiation exposure compared to chest X-ray and chest CT that are commonly employed in the diagnostic work-up of these patients. Additionally, there is a high-risk

of disease transmission to the staff and other patients who have been in contact with the patient.<sup>43–45</sup>

However, in the era of COVID-19, all PET studies, no matter what the clinical indication is, should be screened by the reading nuclear radiologists for COVID-19. In fact, the interpretation of PET/CT should not be restricted to the assessment of neoplastic disease. With the growing incidence of SARS-CoV-2 pneumonia, radiologists and nuclear medicine physicians interpreting PET/CTs and PET/MRIs should be educated about the imaging features of COVID-19 on molecular imaging. COVID-19 should be considered among the differential diagnoses of suspicious imaging features, such as hypermetabolic pulmonary infiltrates and mediastinal and hilar lymphadenopathy, for which constant vigilance is crucial. More specifically, due to atypical clinical features of COVID-19 infection in immunocompromised or high-risk patients, the detection of SARS-CoV-2 pneumonia on PET imaging is of paramount clinical importance.<sup>46</sup>

Furthermore, these patients are more prone to developing complications related to SARS-CoV-2 infection, with increased rates of hospital admissions and mortality, stressing the need for early detection and management of SARS-CoV-2 pneumonia in this high-risk population. The detection of incidental COVID-19 pneumonia in FDG-PET/CT findings has been common in recent studies.<sup>16,17,23</sup> However, the reports are so limited and sparse, and a comprehensive review of these manifestations is still lacking. Here, we systematically reviewed PET/CT findings in the available published articles describing incidental SARS-CoV-2 pneumonia features. To the best of our knowledge, this is the first systematic review in this regard. We found bilateral GGOs, consolidation, and interlobular thickening as the most common CT features in COVID-19 PET/CT imaging, consistent with previous radiologic reports.<sup>47,48</sup> Furthermore, these pulmonary lesions displayed increased FDG uptake, which is not

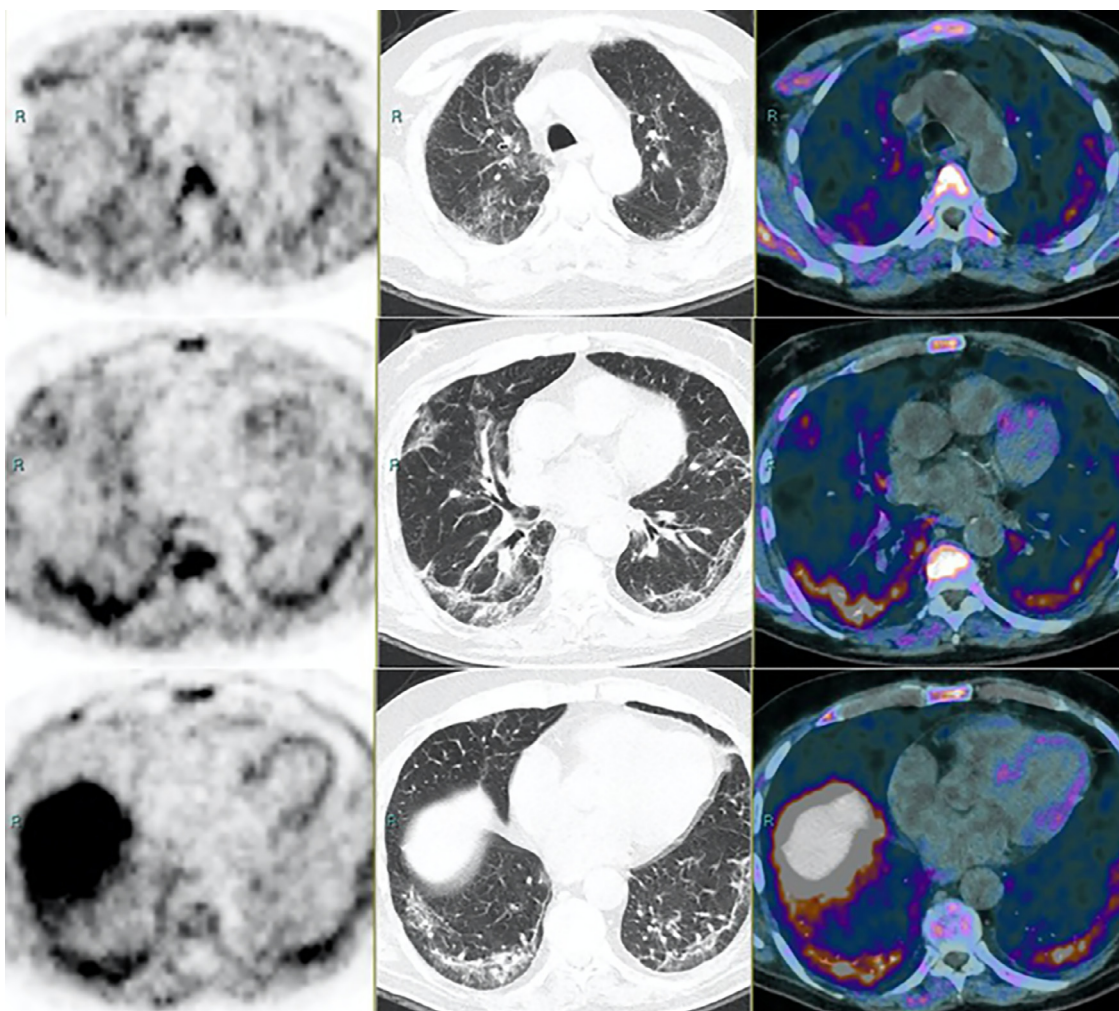


**Figure 4** PET (left panel), CT (middle), and 18-Fluorocholine PET/CT (right) of patient no. 22. First row: upper lung. Second row: middle lung. Third row: lower lung. The patient underwent examination within his routine follow-up for a prostate adenocarcinoma. PSA was 1.97 ng/mL and unchanged compared with the previous evaluation. The CT scan shows diffuse wide areas of solid-subsolid ground-glass opacities, bilateral and subpleural crazy-paving bronchovascular thickening. The patient referred with mild fever ( $>38^{\circ}\text{C}$ ), cough, fatigue, shortness of breath, ageusia-dysgeusia, and anosmia, all strongly suggestive symptoms for a Covid-19 infection. PET shows multiple irregular foci of mild to intense increased FDG uptake, corresponding to consolidations on CT. Images obtained from Savelli et al.,<sup>17</sup> *Medical Hypotheses*, November 2020, Vol. 144(2020):109885, and permission to use granted by Elsevier and Copyright Clearance Center.

unexpected, as acute pneumonia is characterized by hypermetabolism in PET imaging. Reported SUVs have ranged from 2.2 to 18, with a mean pulmonary lesions SUVmax of 4.9. In those cases which demonstrate significantly high metabolic activity, we could suggest follow-up imaging to complete resolution of hypermetabolic space occupying pulmonary lesions to exclude underlying neoplastic lesions.

Sufficient evidence about the potential utility of FDG-PET/CT in the diagnosis and management of infectious and inflammatory diseases already exists.<sup>49</sup> Increased glycolytic activity in the inflammatory cells enables FDG-PET to identify active inflammation sites throughout the body. Besides, the acute infectious process in COVID-19 could also be mapped via PET imaging in patients with immunocompromising underlying diseases, such as cancers.

Additionally noted, even in the absence of nodal enlargement by size criteria of anatomic imaging, increased tracer uptake was frequently seen in the mediastinal and hilar lymph nodes of COVID-19 patients. This suggests that SARS-CoV-2 pneumonia causes lymphadenitis presenting with increased FDG uptake, which contradicts previous radiologic studies about rare nodal involvement in COVID-19 pneumonia.<sup>50,51</sup>

Moreover, the extrapulmonary findings of COVID-19 have been reported recently in literature, causing complications in the brain, gastrointestinal tract, heart and kidneys.<sup>52,53</sup> In this era, a unique advantage of whole-body PET/CT over competing imaging modalities is the potential for detection of additional incidental metabolically active lesions throughout the rest of the body in a single acquisition. Karimi et al<sup>18</sup>

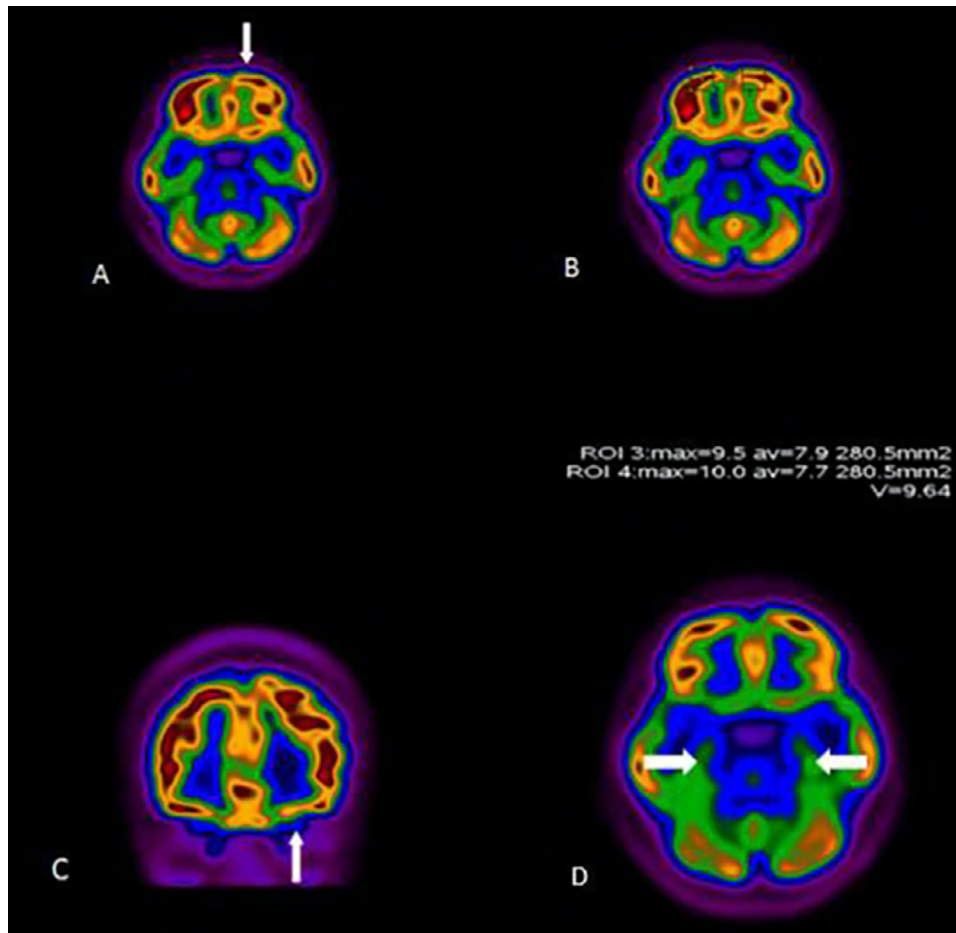


**Figure 5**  $^{18}\text{F}$ -FDG-PET/CT scan of a 27-year-old woman (patient no. 34) with persistent anosmia and positive PCR for SARS-CoV-2. Representative axial (A, B, D) and coronal (C) images are shown. There was decreased uptake in the left orbitofrontal cortex (arrows). The uptake of temporal lobes was symmetric and normal (arrows, D). Images obtained from Karimi-Galougahi et al,<sup>18</sup> *Academic Radiology*, July 2020, Vol. 27(7):1042-1043, and permission to use granted by Elsevier and Copyright Clearance Center.

(no. 34) have reported reduced activity in the orbitofrontal cortex in COVID-19-associated anosmia, which might indicate an impaired neural function as the underlying pathology of anosmia, due to SARS-CoV-2 neurotropism. Also, Zou et al<sup>16</sup> (no. 51) reported bone marrow uptakes in COVID-19, similar to the previous reports of Middle East respiratory syndrome in nonhuman models.<sup>54</sup> This suggests that FDG-PET might be able to assess the end-organ damages of COVID-19. Increased uptake of COVID-19 pulmonary lesions is not limited to FDG-PET studies. Other radiopharmaceuticals have also shown mild increased activity in the pulmonary lesions and lymphadenopathy of COVID-19. Scarlattei et al<sup>39</sup> reported cases (no. 44 and no. 45) of mildly increased activity of pulmonary consolidation in  $^{68}\text{Ga}$ -PSMA (SUVmax of 3.2). They also reported mildly increased uptake of pulmonary consolidation (SUVmax of 3.8) and reactive mediastinal lymphadenopathy (SUVmax of 3.4) in  $^{18}\text{F}$ -choline study.

As mentioned above, FDG-PET/CT holds an important role in monitoring the disease activity, and response evaluation of lung inflammatory pathologies. Deng et al<sup>55</sup> suggested

that higher FDG uptake in pulmonary lesions is positively correlated with both longer healing time and the erythrocyte sedimentation rate value. They reported a patient with a pulmonary lesions SUVmax of 4.6 recovered faster than a patient with a SUVmax of 12.2 (17 days compared to 26 days after the symptom onset). However, these case findings should be confirmed in larger studies before drawing a definite conclusion. Due to some disadvantages of PET imaging as mentioned above, no serial PET imaging is also present to date. However, it is believed that molecular imaging with PET is potentially able to quantify the lung inflammation during the course treatment of lung inflammatory diseases.

Our study has some limitations. First, since per the international guidelines, the elective nuclear medicine operations are not usually performed in patients with confirmed COVID-19, and most of the current reports on the detection of COVID-19 in molecular imaging studies have been obtained in asymptomatic cases. Hence, the imaging manifestations of patients with known infection and/or severe complications have not been studied yet. Second, the limited

**Table 1** Characteristics of 52 Patients With COVID-19 Infection According to Pulmonary and Extrapulmonary PET/CT Imaging Findings

<b>Patient No./ Sex/Age (y)</b>	<b>First Author</b>	<b>Country</b>	<b>Cancer Disease</b>	<b>Radiotracer Type</b>	<b>Extrapulmonary Findings (PET/CT Scan)</b>	<b>Pulmonary Findings (PET/CT Scan)</b>
P1/F/65	Castanheira <sup>19</sup>	Portugal	Breast cancer	<sup>18</sup> F-FDG	Ipsilateral hilar and subcarinal FDG-avid (SUVmax range: 4-5) LN	Unilateral and peripheral GGOs, Rt. Lower lobe interlobular thickening
P2/M/57	Li <sup>20</sup>	China	NR	<sup>18</sup> F-FDG	Normal-sized LN in the mediastinum but with increased metabolic activity	Focal GGOs and bandlike opacities in both lungs without increased metabolic activity
P3/F/58	Amin <sup>12</sup>	Canada	Hodgkin's lymphoma	<sup>18</sup> F-FDG	NR	Multifocal and bilateral peripheral GGOs, moderate <sup>18</sup> F-FDG activity (SUVmax:4.5) in Lt. lower lobe
P4/F/56	Doroudinia <sup>13</sup>	Iran	NR	<sup>18</sup> F-FDG	NR	Bilateral and diffuse GGOs with increased metabolic activity, few bilateral hypermetabolic nodules
P5/M/60	Mo <sup>21</sup>	USA	SCC of tonsil	<sup>18</sup> F-FDG	Foci of hilar and mediastinal FDG avidity	Irregular bilateral GGOs
P6/M/55	Loforte <sup>22</sup>	Italy	NR	<sup>18</sup> F-FDG	NR	Multilobular and subpleural GGOs and consolidation in Rt. and Lt. inferior lobes (SUVmax:10.3-10.6)
P7/M/75	Kamani <sup>23</sup>	Switzerland	NR	<sup>18</sup> F-FDG	Hypermetabolic lymphadenopathy in the Rt. lower paratracheal, subcarinal, and bilateral hilar stations (SUVmax:6.1)	Bilateral, hypermetabolic (SUVmax:7.6) focal GGOs with partial consolidation
P8/M/37	Liu <sup>24</sup>	China	NR	<sup>18</sup> F-FDG	NR	Multiple bilateral <sup>18</sup> F-FDG uptake, GGOs: at apical segment of left and right upper lobes and posterior segment of Lt. upper lobe
P9/M/57	Qin <sup>25</sup>	China	NR	<sup>18</sup> F-FDG	NR	Peripheral GGOs with increased <sup>18</sup> F-FDG uptake (SUVmax range:2.2-4.6) in Rt. upper lung
P10/M/56	Qin <sup>25</sup>	China	NR	<sup>18</sup> F-FDG	Multiple FDG-avid LN in the mediastinum and the subclavian region (SUVmax range: 4.1-7.0)	Multiple FDG-positive GGOs (SUVmax range:7.9-18) in both lungs
P11/F/61	Qin <sup>25</sup>	China	NR	<sup>18</sup> F-FDG	Multiple FDG-positive LN in the mediastinum and the Rt. subclavian region (SUVmax range: 3.4-5.4)	Multiple peripheral FDG-avid GGOs (SUVmax range: 3.7-12.2) in Rt. lung
P12/F/48	Qin <sup>25</sup>	China	NR	<sup>18</sup> F-FDG	Multiple FDG-positive LN in the mediastinum and Rt. hilar region (SUVmax range: 3.8-5.5)	Peripheral FDG-avid GGOs (SUVmax range: 3.7-9.3) with bilateral interlobular septal thickening
P13/NR/53	Czernin <sup>26</sup>	Germany	Pancreatic cancer (NET)	<sup>18</sup> F-FDG	NR	Hypermetabolic area in Rt. upper and lower lobe (SUVmax: 5.5)
P14/F/56	Albano <sup>27</sup>	Italy	Rectal cancer	<sup>18</sup> F-FDG	NR	Bilateral <sup>18</sup> F-FDG-positive GGOs and consolidation, most pronounced in the inferior lobes
P15/M/77	Albano <sup>27</sup>	Italy	Laryngeal cancer	<sup>18</sup> F-FDG	NR	Bilateral faint <sup>18</sup> F-FDG uptake in GGOs (not suggestive of aspiration)
P16/F/55	Albano <sup>27</sup>	Italy	Breast cancer (invasive ductal)	<sup>18</sup> F-FDG	NR	Retrosternal <sup>18</sup> F-FDG-avid nodal relapse, GGOs in the posterior segments of the inferior lung lobes

Table 1 (Continued)

Patient No./ Sex/Age (y)	First Author	Country	Cancer Disease	Radiotracer Type	Extrapulmonary Findings (PET/CT Scan)	Pulmonary Findings (PET/CT Scan)
P17/F/55	Albano <sup>27</sup>	Italy	Hodgkin's lymphoma	<sup>18</sup> F-FDG	Metabolically active lymphoma in the axillary LN	New interstitial opacities near the pleura of the Rt. lung
P18/M/65	Albano <sup>27</sup>	Italy	Laryngeal cancer	<sup>18</sup> F-FDG	NR	Several GGOs with increased FDG uptake (SUVmax: 5.3) in Rt. lung
P19/F/65	Albano <sup>27</sup>	Italy	Ovarian cancer	<sup>18</sup> F-FDG	<sup>18</sup> F-FDG-avid mediastinal LN	Consolidative areas in both lungs with increased <sup>18</sup> F-FDG uptake
P20/F/79	Albano <sup>27</sup>	Italy	Thyroid carcinoma (poorly differentiated)	<sup>18</sup> F-FDG	NR	New diffuse interstitial pneumonia with peripheral GGOs
P21/M/75	Sherman <sup>28</sup>	USA	Non-Hodgkin's lymphoma	<sup>18</sup> F-FDG	FDG-avid thoracic LN	Bilateral FDG-avid peripheral GGOs, multilobar consolidations
P22/NR/NR	Savelli <sup>17</sup>	Italy	Prostate adenocarcinoma	<sup>18</sup> F-choline	ageusia-dysgeusia and anosmia	Multiple irregular foci of increased FDG uptake
P23/M/73	Polverari <sup>29</sup>	Italy	NSCLC	<sup>18</sup> F-FDG	Increased <sup>18</sup> F-FDG uptake involving the Rt. lower paratracheal LN (SUVmax: 5.6)	Bilateral diffuse and intense FDG uptake (SUVmax: 5.9) in Rt. the lower and Lt. lower lobe (SUVmax: 7.9)
P24/M/82	Amini <sup>30</sup>	Iran	Colon cancer (adenocarcinoma)	<sup>18</sup> F-FDG	Hypermetabolic mediastinal LN (SUVmax:4.5)	FDG activity in the Lt. lung (SUVmax range:1.5-8.6) and in the Rt. lung (SUV max range: 1.2-8.3)
P25/M/59	Reed-Embleton <sup>31</sup>	UK	Gastrointestinal stromal tumor	<sup>18</sup> F-FDG	NR	FDG-avid prominently bilateral and peripheral GGOs in upper and lower lobes
P26/F/56	Chuang <sup>32</sup>	USA	SCC	<sup>18</sup> F-FDG	NR	New bilateral multifocal hypermetabolic GGOs
P27/M/59	Olivari <sup>33</sup>	Italy	Recurrent prostate cancer	<sup>18</sup> F-choline	NR	Bilateral subsegmental peripheral GGOs with increased choline uptake (SUV max range: 3–4)
P28/F/45	Setti <sup>34</sup>	Italy	Colon cancer	<sup>18</sup> F-FDG	Modest mediastinal LN uptake	Consolidative opacities
P29/M/67	Setti <sup>34</sup>	Italy	Rectal cancer (adenocarcinoma)	<sup>18</sup> F-FDG	NR	GGOs
P30/F/44	Setti <sup>34</sup>	Italy	Salivary gland carcinoma	<sup>18</sup> F-FDG	Faint mediastinal LN uptake	Consolidative opacities and GGOs
P31/F/56	Setti <sup>34</sup>	Italy	Ovarian carcinoma (clear cell)	<sup>18</sup> F-FDG	NR	GGOs
P32/M/70	Setti <sup>34</sup>	Italy	SCC of lung	<sup>18</sup> F-FDG	NR	GGOs
P33/M/78	Zanoni <sup>35</sup>	Italy	Non-Hodgkin's lymphoma	<sup>18</sup> F-FDG	Multiple FDG avid Lymphadenopathy above and below the diaphragm	Faint and diffuse uptake within a Lt. inferior lobe consolidation and a single non-FDG-avid peripheral rounded GGOs in the Rt. upper lobe

Table 1 (Continued)

Patient No./ Sex/Age (y)	First Author	Country	Cancer Disease	Radiotracer Type	Extrapulmonary Findings (PET/CT Scan)	Pulmonary Findings (PET/CT Scan)
P34/F/27	Karimi-Galougahi <sup>18</sup>	Iran	NR	<sup>18</sup> F-FDG	Lt. orbitofrontal cortex hypometabolism asymmetric confirmed to the lateral side. (SUVmax of 9.5 on the left cortex compared to 10 on the contralateral side)	NR
P35/M/73	Kirienko <sup>36</sup>	Italy	Vascular tumor of retroperitoneum	<sup>18</sup> F-FDG	NR	Increased FDG uptake in the lungs
P36/F/52	Playe <sup>37</sup>	France	Non-Hodgkin's lymphoma (MCL)	<sup>18</sup> F-FDG	Thoracic and subdiaphragmatic LN involvement with high FDG uptake (SUVmax:8.7)	Bilateral GGOs and curvilinear opacities, with predominance in the posterior subpleural areas associated with a moderate FDG uptake (SUVmax: 4)
P37/M/54	Colandrea <sup>38</sup>	Italy	Non-Hodgkin's lymphoma	<sup>18</sup> F-FDG	Multiple FDG-avid LN in mediastinum and Lt. subclavian region	Intense <sup>18</sup> F-FDG uptake on multiple bilateral subsegmental peripheral patchy GGOs with obscure boundaries and mainly subpleural distribution and areas of focal consolidation in the upper lobes
P38/M/61	Colandrea <sup>38</sup>	Italy	Lung and brain tumors (unknown origin)	<sup>18</sup> F-FDG	Multiple FDG-positive areas in mediastinal, subcarinal and hilar LN	Intense <sup>18</sup> F-FDG uptake on multiple peripheral GGOs in the Lt. lower lobe and areas of focal consolidation in the upper lobes
P39/M/48	Colandrea <sup>38</sup>	Italy	Lung cancer (stage IV)	<sup>18</sup> F-FDG	Radiotracer uptake in the treated LN, due to the recent radiotherapy	Intense FDG uptake in a focal consolidation in the upper Lt. lobe, multiple peripheral GGOs with interstitial thickening and thin fibrous stripes in the Lt. lower lobe
P40/M/54	Colandrea <sup>38</sup>	Italy	Cheek melanoma	<sup>18</sup> F-FDG	NR	Intense uptake of subpleural pseudo nodular thickenings in the Rt. lower lobe, multiple small subpleural GGOs and opacities bilaterally without <sup>18</sup> F-FDG uptake
P41/NR/NR	Colandrea <sup>38</sup>	Italy	Tongue carcinoma	<sup>18</sup> F-FDG	Focal FDG-positive area in Rt. hilar LN	Intense <sup>18</sup> F-FDG uptake on multiple peripheral GGOs in both lower lobes and area of focal consolidation in the Rt. upper lobe
P42/M/80	Scarlattei <sup>39</sup>	Italy	Solid lung nodule	<sup>18</sup> F-FDG	Active tracer uptake in Rt. hilar LN (SUVmax:2.5)	Increased tracer uptake (SUVmax: 2.6) corresponding to GGOs in the superior segment of the Lt. lobe with bronchovascular thickening showing mild tracer uptake (SUVmax: 2.5)
P43/F/57	Scarlattei <sup>39</sup>	Italy	Breast cancer (intraductal)	<sup>18</sup> F-FDG	High intensity of tracer uptake in mediastinal, hilar, and carinal LN (SUVmax: 7)	Intense and diffuse uptake (SUVmax range in the Rt. Lung: 2.2-7.7; SUVmax range in the Lt. lung: 2.7-9.1) in both lungs corresponding to GGOs on CT images
P44/M/65	Scarlattei <sup>39</sup>	Italy	Prostate cancer (adenocarcinoma)	<sup>68</sup> Ga-PSMA	NR	Mild tracer uptake (SUVmax: 3.2) in the subpleural region of both lungs, with greater extent in the Rt. lung, corresponding to CT findings of subpleural GGOs in the dependent lung

Table 1 (Continued)

Patient No./ Sex/Age (y)	First Author	Country	Cancer Disease	Radiotracer Type	Extrapulmonary Findings (PET/CT Scan)	Pulmonary Findings (PET/CT Scan)
P45/M/70	Scarlattei <sup>39</sup>	Italy	Prostate cancer (adenocarcinoma)	<sup>18</sup> F-choline	Focal tracer uptake in a hilar, carinal, and peribronchial LN (SUVmax: 3.4)	Mild focal tracer uptake (SUVmax: 3.8) in the subpleural region of both lungs and single GGOs localized in the middle lobe of the right lung
P46/F/57	Scarlattei <sup>39</sup>	Italy	Focal Splenic lesions	<sup>18</sup> F-FDG	NR	Intense/moderate uptake (SUVmax range: 4.6-3.7) in the bilateral subpleural regions corresponding to CT findings of GGOs in the posterior segments
P47/NR/NR	Ajuria-Illarramendi <sup>40</sup>	Spain	Lung cancer	<sup>18</sup> F-FDG	NR	Heterogeneous GGOs with air bronchogram in the superior segment of the Rt. lower lobe with mild diffuse metabolic uptake (SUVmax: 3.9)
P48/NR/NR	Ajuria-Illarramendi <sup>40</sup>	Spain	Lung cancer	<sup>18</sup> F-FDG	NR	Paramedial consolidation and thickened interlobular septa in the Rt. lower lobe with high focal <sup>18</sup> F-FDG avidity (SUVmax: 5.3)
P49/NR/NR	Ajuria-Illarramendi <sup>40</sup>	Spain	Lung cancer	<sup>18</sup> F-FDG	NR	Bibasilar opacities and fibrotic stripes with heterogeneous high metabolic activity (SUVmax:5)
P50/M/67	Martineau <sup>41</sup>	Canada	Lung cancer (adenocarcinoma)	<sup>18</sup> F-FDG	Bilateral, hypermetabolic mediastinal lymphadenopathy, suggestive of reactive LN than metastatic disease	Relatively intense uptake (SUVs range:5.0-7.2) in the peripheral opacities
P51/M/55	Zou <sup>16</sup>	China	Suspect hilar malignancy	<sup>18</sup> F-FDG	Increased FDG uptake of the Rt. paratracheal and Rt. hilar LN as well as bone marrow	FDG-avid mass (SUVmax:4.9) in the Rt. Lung. The GGOs with areas of focal consolidation primarily in the Rt. upper lobe and focal opacities in the Lt. upper and Rt. middle lobes
P52/M/87	Krebs <sup>42</sup>	USA	Primary salivary duct carcinoma	<sup>18</sup> F-FDG	NR	Multiple areas of FDG-avid GGOs and patchy opacities with interlobular septal thickening in both lungs

GGOs, ground-glass opacities; LN, lymph node; Lt., left; MCL, mantle cell lymphoma; NET, neuroendocrine tumor; NR, not reported; NSCLC, non-small-cell lung cancer; Rt., right; SCC, squamous cell carcinoma; SUV, standardized uptake values (all reported based on g/mL).

**Table 2** Types of Cancer in Study Patients

Cancer Type (Subtypes)	Number of Patients
Breast cancer (invasive ductal, intraductal)	3
Hodgkin's lymphoma	2
Non-Hodgkin's lymphoma (mantle cell lymphoma)	4
Squamous cell carcinoma (tonsil, paratracheal lymph node)	2
Pancreas tumor (NET*)	1
Rectal cancer (adenocarcinoma of rectum, primary staging tumor)	2
Laryngeal cancer	2
Ovarian cancer (clear cells ovary carcinoma)	2
Thyroid carcinoma (poorly differentiated)	1
Prostate cancer	4
Colon adenocarcinoma	2
Gastrointestinal stromal tumor (GIST)	1
Salivary carcinoma (duct, gland carcinoma)	2
Vascular tumor of retroperitoneum	1
Lung cancer (NSCLC <sup>#</sup> , adenocarcinoma)	8
Cheek melanoma	1
Tongue carcinoma	1
<b>Total</b>	<b>39</b>

\*NET, neuroendocrine tumor.

<sup>#</sup>NSCLC, non-small-cell lung cancer.

**Table 3** Types of Lymph Node Involvement in Study Patients

Lymph Node Type	Number of Patients
Hilar	10
Subcarinal	5
Mediastinal	14
Subclavian	3
Paratracheal	3
Thoracic	2
Subdiaphragmatic	2
<b>Total</b>	<b>39</b>

number of reports in this era might limit the interpretation, and thus further studies are warranted.

Overall, the potential value of PET imaging to better understand and characterize the disease might help us improve our coping strategies during this ongoing pandemic. However, although contested by many the fact that PET can be a noninvasive beneficial imaging tool in the early detection and monitoring COVID-19 pneumonia in high-risk patients, we believe that PET should not be recommended in the diagnostic work-up of COVID-19 and other infectious types of pneumonia, as poses the risk of the disease spreading in nuclear medicine units and other imaging modalities are available that can provide sufficient clinical and diagnostic information.<sup>56</sup> Thus, more investigations with modified protocols are needed in future, to fully explore the possible clinical indications of molecular imaging for characterizing the

disease severity and its prognosis.<sup>57</sup> Incidental detection of different abnormalities in nuclear medicine studies has been widely discussed in the literature. Accordingly, we strongly recommend the evaluation of PET images for previously unsuspected pathologies in daily practice, as this may eventually lead to uncovering of crucial pathologies that significantly change the patient management and prognosis. This is particularly important with the evolving diseases of the 21st century.<sup>45,46,58</sup>

## Conclusion

This systematic review gains a deep insight over the diagnostic value of detecting COVID-19 on PET imaging performed for other clinical indications. As patients undergoing PET imaging usually suffer from immunocompromising underlying diseases, such as cancers, early detection of potentially life-threatening and devastating pneumonia in these patients is of paramount importance to minimize the disease complications and limit the progression. This not only helps to uncover clinically unsuspected COVID-19 in this sensitive population, but also helps ensure appropriate postexposure precautions are implemented for the department and hospital staff and those who have been in contact with the patient.

## Conflicts of Interest

The authors declare that they have no conflict of interest.

## Informed Consent

Informed consent was not required because it was a literature study.

## Ethical Approval

Institutional Review Board approval was not required because it was a literature study.

## Authors' Contributions

All authors designed the study and wrote the manuscript. FR, PK, SFN, FE performed literature research. FR, PK, AGH conducted manuscript editing. FR, PK, and AGH significantly supported conception and design of the study.

## Acknowledgments

The authors would like to thank Dr S. Zou, Dr G. Savelli, and Dr M. Karimi-Galougahi for providing the images and figures for this study and also, thank to publisher holder of *Radiology (RSNA)*, *Medical Hypotheses*, and *Academic Radiology Journal* for granting permission to use the images.

## Supplementary materials

Supplementary material associated with this article can be found, in the online version, at [doi:10.1053/j.semnuclmed.2020.10.002](https://doi.org/10.1053/j.semnuclmed.2020.10.002).

## References

- Yang X, Yu Y, Xu J, et al: Clinical course and outcomes of critically ill patients with SARS-CoV-2 pneumonia in Wuhan, China: A single-centered, retrospective, observational study. *Lancet Resp Med* 8:475-481, 2020
- Organization WH: Coronavirus Disease (COVID-19) Situation Reports. 2020 Available at: <https://www.who.int/emergencies/diseases/novel-coronavirus-2019/situation-reports/>. Accessed July 23, 2020
- Salehi S, Abedi A, Balakrishnan S, et al: Coronavirus disease 2019 (COVID-19): A systematic review of imaging findings in 919 patients. *AJR Am J of Roentgenol* 250:87-93, 2020
- Ai T, Yang Z, Hou H, et al: Correlation of chest CT and RT-PCR testing in coronavirus disease 2019 (COVID-19) in China: A report of 1014 cases. *Radiology* 293:E2-E40, 2020
- Ashraf MA, Keshavarz P, Hosseinpour P, et al: Coronavirus disease 2019 (COVID-19): a systematic review of pregnancy and the possibility of vertical transmission. *J Reprod Infertil* 21:157-168, 2020
- Katal S, Aghaghazvini L, Gholamrezaezhad A: Chest-CT findings of COVID-19 in patients with pre-existing malignancies; a pictorial review. *Clin Imaging* 67:121-129, 2020
- Ye Z, Zhang Y, Wang Y, et al: Chest CT manifestations of new coronavirus disease 2019 (COVID-19): A pictorial review. *Eur Radiol* 30:4081-4089, 2020
- Salehi S, Reddy S, Gholamrezaezhad A: Long-term pulmonary consequences of coronavirus disease 2019 (COVID-19): What we know and what to expect. *J Thorac Imaging* 35:W87-W89, 2020
- Manna S, Wruble J, Maron SZ, et al: COVID-19: A multimodality review of radiologic techniques, clinical utility, and imaging features. *Radiol: Cardiothorac Imaging* 2:e200210, 2020
- Haroon A, Zumla A, Bomanji J: Role of fluorine 18 fluorodeoxyglucose positron emission tomography-computed tomography in focal and generalized infectious and inflammatory disorders. *Clin Infect Dis* 54:1333-1341, 2020
- Giraud C, Evangelista L, Fraia AS, et al: Molecular imaging of pulmonary inflammation and infection. *Int J Mol Sci* 21:894-915, 2020
- Amin R, Grinblat L, Husain M: Incidental COVID-19 on PET/CT imaging. *CMAJ* 192, 2020. E631-E
- Doroudinia A, Tavakoli M: A case of coronavirus infection incidentally found on FDG PET/CT scan. *Clin Nucl Med* 45:e303-e304, 2020
- aBlw NHL. Study Quality Assessment Tools. Available at: <http://www.nhlbi.nih.gov/health-topics/study-quality-assessment-tools>. Accessed 6 April 2020.
- Margulis AV, Pladevall M, Riera-Guardia N, et al: Quality assessment of observational studies in a drug-safety systematic review, comparison of two tools: the Newcastle-Ottawa scale and the RTI item bank. *Clin Epidemiol* 6:359-365, 2014
- Zou S, Zhu X: FDG PET/CT of COVID-19. *Radiology* 296:E118, 2020
- Savelli G, Bonacina M, Rizzo A, et al: Activated macrophages are the main inflammatory cell in COVID-19 interstitial pneumonia infiltrates. Is it possible to show their metabolic activity and thus the grade of inflammatory burden with 18F-Fluorocholine PET/CT. *Med Hypotheses* 144:109885, 2020
- Karimi-Galougahi M, Yousefi-Koma A, Bakhshayeshkaram M, et al: 18FDG PET/CT scan reveals hypoactive orbitofrontal cortex in anosmia of COVID-19. *Acad Radiol* 27:1042-1043, 2020
- Castanheira J, Gaivão AM, Teixeira SM, et al: Asymptomatic COVID-19 positive patient suspected on FDG-PET/CT. *Nucl Med Commun* 41:598-599, 2020
- Li X, Wang Y, Bai Y, et al: PET/MR and PET/CT in a severe COVID-19 patient. *Eur J Nucl Med Mol Imaging* 47:2078-2079, 2020
- Mo A, Brodin NP, Tomé WA, et al: COVID-19 incidentally detected on PET/CT during work-up for locally advanced head and neck cancer. *In Vivo* 34(3 suppl):1681-1684, 2020
- Loforte A, Gliozzi G, Suarez SM, et al: Positron emission tomography for detecting COVID-19 in asymptomatic left ventricular assist device recipients. *Asaio J* 66:599-602, 2020
- Kamani CH, Jreige M, Pappon M, et al: Added value of 18F-FDG PET/CT in a SARS-CoV-2-infected complex case with persistent fever. *Eur J Nucl Med Mol Imaging* 47:2036-37:2036-2037, 2020
- Liu C, Zhou J, Xia L, et al: 18F-FDG PET/CT and serial chest CT findings in a COVID-19 patient with dynamic clinical characteristics in different period. *Clin Nucl Med* 45:495-496, 2020
- Qin C, Liu F, Yen T-C, et al: 18 F-FDG PET/CT findings of COVID-19: A series of four highly suspected cases. *Eur J Nucl Med Mol Imaging* 47:1281-1286, 2020
- Czernin J, Fanti S, Meyer PT, et al: Nuclear medicine operations in the times of COVID-19: Strategies, precautions, and experiences. *J Nucl Med* 61:626-629, 2020
- Albano D, Bertagna F, Bertoli M, et al: Incidental findings suggestive of COVID-19 in asymptomatic patients undergoing nuclear medicine procedures in a high-prevalence region. *J Nucl Med* 61:632-636, 2020
- Sherman FT, Lechich AJ: Nursing home physician with normal chest X-ray and probable COVID-19 based on 18F-FDG PET/CT imaging. *J Am Geriatr Soc* 68:1918-1920, 2020
- Polverari G, Arena V, Ceci F, et al: 18F-fluorodeoxyglucose uptake in patient with asymptomatic severe acute respiratory syndrome coronavirus 2 (coronavirus disease 2019) referred to positron emission tomography/computed tomography for NSCLC restaging. *J Thorac Oncol* 15:1078-1080, 2020
- Amini H, Divband G, Montahaei Z, et al: A case of COVID-19 lung infection first detected by [18F] FDG PET-CT. *Eur J Nucl Med Mol Imaging* 47:1771-1772, 2020
- Reed-Embleton H, Khan KS, Mathias N, et al: Case report: Incidental findings of COVID-19 infection on positron emission tomography/computed tomography for staging of a giant gastric gastrointestinal stromal tumour. *Pan Afr Med J* 35:28, 2020
- Chuang HH, Emery DJ, Campbell RM, et al: FDG PET/CT in diagnosing COVID-19 infection in a cancer patient with exposure history but minimal symptoms. *Clin Nucl Med* 45:656-658, 2020
- Olivari L, Riccardi N, Rodari P, et al: COVID-19 pneumonia: Increased choline uptake with 18F-choline PET/CT. *Eur J Nucl Med Mol Imaging* 47:2476-2477, 2020
- Setti L, Kirienko M, Dalto SC, et al: FDG-PET/CT findings highly suspicious for COVID-19 in an Italian case series of asymptomatic patients. *Eur J Nucl Med Mol Imaging* 47:1649-1656, 2020
- Zanoni L, Mosconi C, Cervati V, et al: [18F]-FDG PET/CT for suspected lymphoma relapse in a patient with concomitant pneumococcal pneumonia during COVID-19 outbreak: Unexpected SARS-Cov-2 co-infection despite double RT-PCR negativity. *Eur J Nucl Med Mol Imaging* 2038-2039, 2020
- Kirienko M, Padovano B, Serafini G, et al: CT,[18F] FDG-PET/CT and clinical findings before and during early Covid-19 onset in a patient affected by vascular tumour. *Eur J Nucl Med Mol Imaging* 47:1769-1770, 2020
- Playe M, Siavellis J, Braun T, et al: FDG PET/CT in a patient with mantle cell lymphoma and COVID-19: Typical findings. *Clin Nucl Med* 45:e305-e306, 2020
- Colandrea M, Gilardi L, Travaini LL, et al: 18F-FDG PET/CT in asymptomatic patients with COVID-19: The submerged iceberg surfaces. *Researchsquare* 38:1007-1011, 2020
- Scarlattei M, Baldari G, Silva M, et al: Unknown SARS-CoV-2 pneumonia detected by PET/CT in patients with cancer. *Tumori* 106:325-332, 2020
- Ajuria-Illarramendi O, Martinez Lorca A, Orduña-Diez M: [18F]FDG-PET/CT in different COVID-19 phases. *IDCases* 21:e00869, 2020
- Martineau P, Kidane B: FDG PET/CT findings in an asymptomatic case of confirmed COVID-19. *Clin Nucl Med* 45:647-648, 2020

42. Krebs S, Petkovska I, Ho AL, et al: Laboratory-proven asymptomatic SARS-CoV-2 (COVID-19) infection on 18F-FDG PET/CT. *Clin Nucl Med* 45:654-655, 2020
43. Van Uden D, Prins M, Siesling S, et al: [18F] FDG PET/CT in the staging of inflammatory breast cancer: A systematic review. *Crit Rev Oncol Hematol* 15:102943, 2020
44. Alavi A, Hess S, Werner TJ, et al: An update on the unparalleled impact of FDG-PET imaging on the day-to-day practice of medicine with emphasis on management of infectious/inflammatory disorders. *Eur J Nucl Med Mol Imaging* 47:18-27, 2020
45. Gholamrezanezhad A, Guermazi A, Salavati A, et al: PET-computed tomography and PET-MR imaging and their applications in the twenty-first century. *PET Clin* 14, 2019. xv-xvii
46. Behzad S, Velez E, Najafi MH, et al: Coronavirus disease 2019 (COVID-19) pneumonia incidentally detected on coronary CT angiogram: a do-not-miss diagnosis. *Emerg Radiol*: 4, 2020
47. Hosseiny M, Kooraki S, Gholamrezanezhad A, et al: Radiology perspective of coronavirus disease 2019 (COVID-19): Lessons from severe acute respiratory syndrome and Middle East respiratory syndrome. *AJR Am J Roentgenol* 214:1078-1082, 2020
48. Hu Q, Guan H, Sun Z, et al: Early CT features and temporal lung changes in COVID-19 pneumonia in Wuhan, China. *Eur J Radiol* 128:109017, 2020
49. Treglia G: Diagnostic performance of 18F-FDG PET/CT in infectious and inflammatory diseases according to published meta-analyses. *Contrast Media Mol Imaging* 2019:1-12, 2019
50. Han R, Huang L, Jiang H, et al: Early clinical and CT manifestations of coronavirus disease 2019 (COVID-19) pneumonia. *AJR Am J Roentgenol* 215:338-343, 2020
51. Wu J, Wu X, Zeng W, et al: Chest CT findings in patients with coronavirus disease 2019 and its relationship with clinical features. *Invest Radiol* 55:257-261, 2020
52. Katal S, Balakrishnan S, Gholamrezanezhad A: Neuroimaging findings in COVID-19 and other coronavirus infections: A systematic review in 116 patients. *Neuroradiology* 922:1-8, 2020
53. Behzad S, Aghaghazvini L, Radmard AR, et al: Extrapulmonary manifestations of COVID-19: Radiologic and clinical overview. *Clin Imaging* 66:35-41, 2020
54. Chefer S, Thomasson D, Seidel J, et al: Modeling [18 F]-FDG lymphoid tissue kinetics to characterize nonhuman primate immune response to Middle East respiratory syndrome-coronavirus aerosol challenge. *Eur J Nucl Med Mol Imaging* 5:1-11, 2015
55. Deng Y, Lei L, Chen Y, et al: The potential added value of FDG PET/CT for COVID-19 pneumonia. *Eur J Nucl Med Mol Imaging* 47:1634-1635, 2020
56. Joob B, Wiwanitkit V: 18F-FDG PET/CT and COVID-19. *Eur J Nucl Med Mol Imaging* 47:1348, 2020
57. Guedj E, Verger A, Cammilleri S: PET imaging of COVID-19: The target and the number. *Eur J Nucl Med Mol Imaging* 47:1636-1637, 2020
58. Gholamrezanezhad A, Mirpour S: An important but easily forgettable review: Extracardiac activity in myocardial perfusion scans. *Int Cardio-vasc Imaging* 23:207-208, 2007